JOURNAL OF GUIDANCE, CONTROL, AND DYNAMICS
Vol. 20, No. 4, July–August 1997

Experimental Verification of Vibration Reduction in Flexible Spacecraft Using Input Shaping

Timothy D. Tuttle* and Warren P. Seering†
Massachusetts Institute of Technology, Cambridge, Massachusetts 02139

The performance of many spacecraft can be improved by using closed-loop control and command-shaping techniques. However, because little information exists about the operation of controlled structures in zero gravity, it is difficult for designers to anticipate and place confidence in the on-orbit performance of their ground-based control designs. To address this issue, the middeck active control experiment was conducted aboard the Space Shuttle Endeavor in March of 1995. The results of the command shaping experiments implemented during the mission are presented, and guidelines for using command shaping to suppress unwanted vibration in flexible space structures are proposed.

I. Introduction

THE combination of stringent performance specifications and lightly damped structural modes makes the effective operation of many space systems vulnerable to vibration. To attack this problem, closed-loop control and open-loop command-shaping techniques are often enlisted. However, with only ground-based testing available prior to on-orbit implementation, uncertainty about zero-gravity (0-g) behavior can hamper the success of these 0-g control designs.

The Massachusetts Institute of Technology (MIT) middeck active control experiment (MACE) is a Space Shuttle flight experiment designed to expose critical issues associated with the design of controllers and shaped commands for 0 g. As part of this experiment, data were collected from a flexible structure on-orbit, and results illustrated that both the control and command-shaping strategies employed on the test article could effectively reduce problematic vibration. Additionally, as a result of careful ground-based modeling efforts, predictions of 0-g behavior were accurate enough to achieve high-performance control and command shaping without on-orbit redesign. After introducing the MIT MACE project and the MACE command-shaping efforts, this paper presents the results from a specific subset of the mission experiments: the MACE input shaping tests. Based on these results, key points are summarized and conclusions are drawn.

II. MACE Project

A. MACE Mission

The purpose of MACE is to develop and verify a set of techniques that can be used to give designers of spacecraft, which cannot be tested adequately on the ground, confidence in eventual on-orbit performance. To achieve this objective, the MACE hardware (Fig. 1) was flown aboard the Space Shuttle Endeavor in March of 1995. As shown in Fig. 1, two different hardware configurations were tested during this mission, and three main tasks were performed on each to investigate modeling and control design in a 0-g environment. First, controllers and shaped inputs, which were designed prior to flight using ground-based modeling efforts, were implemented. Second, a system identification (ID) was performed on-orbit, and the resulting ID data were downlinked and used to formulate new controllers and shaped inputs. Last, these new controllers and inputs were uplinked during the mission and implemented on the MACE hardware. A more detailed overview of the MACE project is available in Ref. 1.

B. MACE Hardware Description

The MACE test article was designed to be representative of a typical precision-controlled, high payload-mass-fraction spacecraft, such as an Earth-observing satellite, with multiple independent scanning or pointing instruments. As a result, the MACE hardware (Fig. 1) consists of a long flexible bus with a gimbal at each end. Actuated by direct-drive dc torque motors, each of the two gimbals can move its payload around two perpendicular axes. The MACE bus is constructed from four tubular polycarbonate struts, one of which contains piezoelectric material to actuate bending strain in the structure. In addition to these actuators, a reaction-wheel assembly is located in the center of the MACE structure to provide attitude control of the test article. This assembly is composed of three orthogonally mounted inertia wheels driven by dc servomotors.

To closely monitor open- and closed-loop performance, the test article is outfitted with a variety of sensors. Specifically, each gimbal axis has a laser rotary encoder to measure the angle of the gimbal relative to the bus. Also, a two-axis rate-gyro platform is mounted on the payload arm of the primary gimbal while a three-axis rate-gyro platform measures bus rotation at the reaction-wheel assembly. Last, eight pairs of strain gauges are mounted on the bus links, two per strut, to monitor the vertical and horizontal bending strains in the structure.

All electronics for collecting sensor data and controlling actuators reside in the MACE experiment support module (ESM). In addition to harboring a digital-signal-processing (DSP)-based real-time control computer to implement control algorithms, the ESM contains analog servos for the reaction wheels, rate-gyro notch filters, and sensor antialiasing filters, as well as all data-acquisition electronics. Using the DSP board and feedback from encoder rate signals, all four gimbal motors are controlled by single input/single output proportional-integral servos. For some experiments, the control computer is also used to send shaped and unshaped disturbance commands to the gimbal actuators while a multi-input/multi-output (MIMO) high-performance controller attempts to regulate the inertial position of the primary gimbal. All controllers are run at a 500-Hz sampling rate.

Prior to flight, configuration 1 of the MACE hardware was ground-tested thoroughly. In an attempt to replicate 0-g behavior in a 1-g environment, the entire structure was supported on a pneumatic-electric active suspension. This suspension supported the structure at the bus center and both ends and was designed to have low-frequency rigid-body modes well below 1 Hz.

C. MACE Modeling

The design of high-performance controllers and shaped inputs for the 0-g MACE tests relied heavily on the development of accurate 0-g models. Because the exact behavior of the MACE structure in

Received May 14, 1996; revision received March 31, 1997; accepted for publication April 5, 1997.

*Research Assistant, Artificial Intelligence Laboratory, Space Engineering Research Center and Department of Mechanical Engineering, Room 828, 545 Technology Square.

†Professor of Mechanical Engineering, Space Engineering Research Center and Department of Mechanical Engineering, Room 3-433, 77 Massachusetts Avenue.

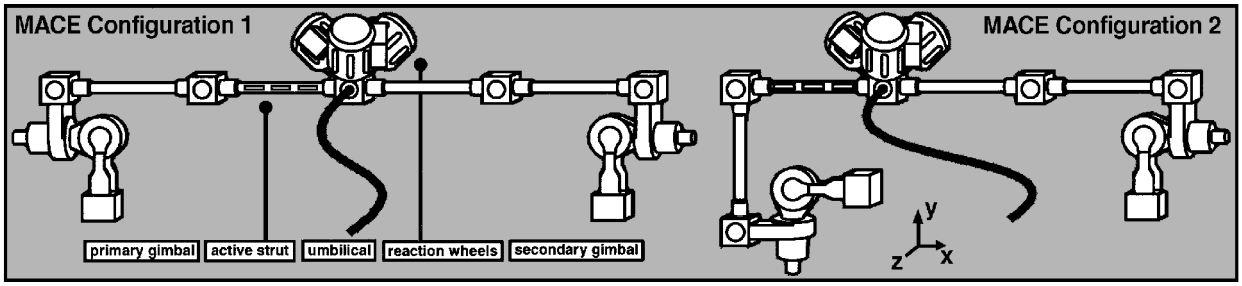

Fig. 1 Schematic of the MACE flight hardware in both configurations.

0 *g* could not be measured prior to flight, a finite element model (FEM) to predict the on-orbit behavior was created using ground-based testing of the flight hardware. Specifically, a parameter-based FEM was developed to replicate the behavior of configuration 1 of the MACE hardware as supported by the active suspension in 1 *g*. The open- and closed-loop behavior of this model was then compared to that of the actual structure to refine the model and verify its validity. When the 1-*g* FEM was sufficiently accurate, the 0-*g* model was created by removing gravity and the suspension system from the 1-*g* model. The resulting 0-*g* model, which contained 130 states and 13 modes below 20 Hz, represented the best available predictor of real on-orbit behavior for MACE configuration 1. The 0-*g* model of MACE configuration 2, like the one of configuration 1, was created from a parameter-based FEM. However, unlike the model of configuration 1, the configuration 2 0-*g* model was never refined using 1-*g* testing data. A detailed account of MACE finite element modeling work can be found in Refs. 2 and 3.

The second aspect of the MACE modeling effort was the creation of measurement-based models using actual on-orbit data. Because these measurement-based models were derived directly from the experimental data, they proved to be highly accurate predictors of system behavior. As a result, they were also used as a baseline from which the accuracy of the 0-*g* FEMs could be measured. In particular, the measurement-based system-ID to be performed on MACE employed the frequency-domain observability range space extraction technique, as described in Ref. 4, to convert frequency-domain data into a state-space system model. During the MACE mission, this algorithm was applied to on-orbit data to create highly accurate 0-*g* models, which were used to design some of the controllers and shapers implemented during the flight. The results of these redesigned experiments were used to understand the value of on-orbit system identification for maximizing 0-*g* performance.

D. MACE Control

The success of MACE was evaluated in part on its ability to exhibit high-performance structural control in a 0-*g* environment. Reaching this goal depended not only on accurate 0-*g* models but also on control-synthesis techniques that were robust to errors in these models. To address this issue, modern MIMO robust-control algorithms, such as sensitivity-weighted linear quadratic Gaussian (LQG) and multiple model control, as described in Refs. 5 and 6, were implemented during the MACE mission. The performance of these controllers was measured by their ability to isolate the primary gimbal from vibrations in the test article excited by the secondary gimbal. Results from these experiments can be found in Ref. 7.

E. MACE Command Shaping

As a second metric for evaluating the success of MACE, command-shaping techniques were employed to reduce problematic vibration in the test article. Unlike the closed-loop control approaches, command shaping (Fig. 2a) is an open-loop or feedforward technique inasmuch as it does not rely on sensor feedback. Instead, command shaping uses modal information from the system model to modify actuator commands to suppress residual vibration and ensure rapid system response. Performance of these command shapers was assessed based on their ability to minimize the settling time of the MACE structure. As a primary candidate for on-orbit evaluation, a command-shaping technique, called input shaping, was

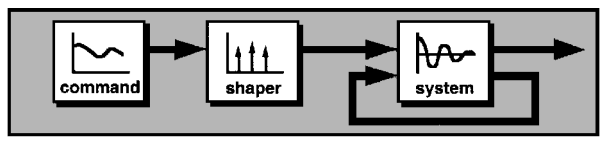

Fig. 2a System with a shaper.

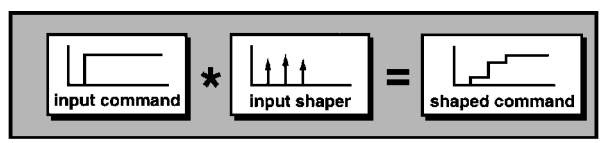

Fig. 2b Creating a shaped command using convolution.

implemented during the mission. The remainder of this paper is dedicated to discussing the goals and results of the MACE input shaping experiments.

III. MACE Input Shaping Experiments

A. Background

Because of their ability to adjust to unforeseen disturbances, closed-loop controllers are often indispensable for ensuring adequate performance. However, in many cases, such as when good closed-loop control is infeasible or when unknown disturbances are minimal, feedforward techniques provide a simple and effective alternative to feedback. Additionally, even with systems that already employ closed-loop control, command shaping methods can typically be used in parallel with the controllers to gain an extra measure of performance.

In the past 20 years, researchers have proposed many methods for creating shaped commands to reduce vibration in flexible space structures. The researchers include Farrenkopf,[8] who used calculus of variations to generate command profiles designed to minimize vibration in a simple flexible spacecraft model. Addressing a similar problem, Swigert[9] proposed a method for minimizing modal vibration in a flexible satellite system by using shaped torque commands constructed from finite trigonometric series. Turner and Junkins[10] considered a model of a spacecraft with flexible appendages and derived command profiles designed to minimize vibration using optimal control techniques. Each of these researchers, as well as many others, demonstrated the potential of feedforward commands for reducing vibration in space-borne systems.

From the many methods that have been proposed for generating spacecraft slewing maneuvers that minimize unwanted vibration, the technique called input shaping has received much attention due to its simplicity and ability to maximize the speed of system response. Input shaping is a strategy for generating shaped commands for controlled mechanical systems using only information about the problematic system modes of vibration. In this approach, shaped commands are created by convolving an actuator command with a series of impulses, called the input shaper (Fig. 2b). The impulse sequence can be derived by numerically solving a set of simple constraint equations or, in some cases, by using a closed-form solution. Singer and Seering[11] first explored this area of research seven years ago, and since then, it has received considerable attention from many researchers, including Magee and Book[12] and Tzes et al.[13] As one of the many explored applications of this technology, the control of

flexible space structures using input shaping has been the subject of much recent research. In particular, Singhose et al.,[14] Singh and Vadali,[15] Liu and Wie,[16] and Rogers[17] proposed strategies for applying input shaping techniques to spacecraft with on-off thruster jets. Banerjee[18] used a similar approach to reduce vibration and deflection in a model of a large space-based antenna. Using a simulation of the Space Shuttle robot arm, Singer and Seering[19] proposed new methods for improving robustness in the theory. In some early work on MACE, Hyde and Seering[20] and Chang[21] used nonlinear simulations and experimental 1-*g* data to reduce multiple-mode vibration in preliminary versions of the MACE test article. In each of these cases and others, input shaping has demonstrated great potential for improving the performance of flexible space-based systems. With the completion of the MACE mission, actual 0-*g* experimental data are available for the first time to verify these results and assess the suitability of input shaping for space-borne systems.

B. Designing Input Shapers for MACE

Input shapers for MACE were designed using time-response simulations produced by the MACE models. From these simulations, modes present in the residual vibration were identified and the input shapers were targeted to eliminate vibration from these modes. For the shapers designed prior to flight, the 0-*g* FEM was used to make modal predictions, and, for the shapers that were designed during flight, vibration modes were determined from the measurement model derived from the on-orbit system identification. When available, down-linked experimental data were used to evaluate and improve shaper performance.

The techniques used to derive the impulse sequences used on MACE are described in Refs. 11, 22, and 23. By convolving these sequences with step commands, shaped commands were generated that reduced residual vibration in the system response. For the most part, the slewing maneuvers implemented on the MACE structure excited only the first one or two structural modes of the MACE hardware, and as a result, most flight experiments used either one or two mode shapers. Also, because the MACE models proved to be accurate predictors of actual on-orbit performance, many of the shapers were designed with the minimum level of robustness to modal uncertainty, referred to as zero-vibration (ZV) robustness.

C. Experimental Approach

The MACE test article was designed to be representative of space systems with pointing and scanning instruments, and consequently, the MACE input shaping experiments incorporated two typical tasks performed by such spacecraft. The first task, called the one-gimbal task, attempted to explore the performance tradeoffs for a single scanning instrument mounted on a flexible space structure. In these one-gimbal experiments, the performance objective was to slew the primary gimbal and bring it to rest in a new position as quickly as possible. Unfortunately, vibrations excited in the MACE structure by the slewing maneuver tended to corrupt the positioning accuracy of the primary gimbal payload. To remedy this problem, commands sent to the primary gimbal were shaped to minimize vibration while ensuring maximum slewing speed. Several different types of shaped slews were implemented during the MACE mission and evaluated based on their ability to minimize the settling time of the primary gimbal payload after a slewing maneuver.

The second task studied during the MACE mission was aimed at understanding how to improve the performance of space systems containing multiple scanning or pointing payloads. Referred to as the two-gimbal task, this type of experiment employed a MIMO controller to regulate the primary gimbal at a constant inertial angle while the secondary gimbal performed slewing maneuvers. Because of the vibrations excited in the structure by the secondary-gimbal motions, the positioning accuracy of the primary gimbal can be compromised. To improve the pointing performance of the primary gimbal by minimizing its settling time, a variety of shaped slews were executed on the secondary gimbal.

For both the one-gimbal and two-gimbal tasks, three different classes of experiments were implemented. First, for each task, experiments were implemented using shapers designed prior to flight, as well as shapers designed after flight data were collected. By comparing the results of these two types of experiments, statements can be made about the benefits of designing shapers using actual 0-*g* experimental data as opposed to 0-*g* predictions. Second, to generalize about ground-based shaper designs for 0-*g*, predictions of 0-*g* behavior were generated using the FEM and compared to actual 0-*g* data. Third, for each task, experiments were evaluated on both configurations 1 and 2 of the test article. Because the configuration 2 model was developed without any ground-based verification or testing, comparing the results of the two types of tests can lend insight into the importance of ground testing for ensuring maximum on-orbit performance. The remainder of this paper is devoted to discussing the mission results for both the one-gimbal and two-gimbal tasks, and in this discussion, observations will be made to address the three issues just outlined. A more detailed discussion of the experimental approach can be found in Ref. 24.

IV. Results for the MACE One-Gimbal Task

A. Experiment Description

As already described, the one-gimbal task involves slewing the MACE primary gimbal and measuring the resulting pointing accuracy upon completion of the move. In these tests, the input command is sent to the primary gimbal z-axis actuator servo, whereas the absolute angle of the primary gimbal z axis, as measured by the rate gyro, is used to record the system response. This section presents and discusses the results of these experiments for both MACE configurations 1 and 2. For all of these results, the settling time is evaluated based on an envelope of ± 0.01 deg around the response final value.

B. Configuration 1 Results

The results from the MACE configuration 1, one-gimbal task are shown in Figs. 3–5. In particular, Fig. 3 illustrates the time response of the primary gimbal that results from four different motion commands: a step command (Fig. 3a), a trapezoidal-velocity-profile command (Fig. 3b), a shaped step designed before flight (BF) (Fig. 3c), and a shaped step designed after a flight system ID (AF) was performed (Fig. 3d). In each of these four plots, both the input command and the experimental response are shown as solid lines and the predicted open-loop response is shown as a dashed line. As plotted, the input command for each test is designed to transition the gimbal angle relative to the bus by 3 deg. Because the gimbal response is measured as an absolute rather than relative angle, the recorded distance of the gimbal slew, as shown in Fig. 3, is slightly less than 3 deg.

As the experimental response in Fig. 3a demonstrates, a step command to the open-loop system excites substantial vibration primarily at the first bending mode of the test article. This residual vibration is so lightly damped that it takes about 20 s for the response to settle within the desired performance envelope of ± 0.01. When a standard trapezoidal velocity profile is used instead (Fig. 3b), the vibration is reduced by two-thirds, but the settling time is still about 16 s. Using the FEM model of configuration 1 to design a 1-mode, ZV input shaper prior to flight, Fig. 3c illustrates that both the settling time and the residual vibration in response to the shaped step are dramatically reduced. Finally, by updating the 1-mode ZV input shaper during the MACE mission to match the measured on-orbit modes, the residual vibration performance is improved slightly (Fig. 3d), but the settling time remains the same.

By comparing the experimental response to the predicted response in Fig. 3, it can be seen that the predicted and actual performance show fairly good agreement. Quantitatively, as best illustrated in Figs. 3a and 3b, the predictions made prior to flight using the FEM indicated that the first bending mode would occur at a frequency of 2.10 Hz with a damping ratio of 0.02. As the experimental results indicate, the actual frequency was measured at 2.19 Hz with a damping ratio of about 0.01. This relatively close agreement accounts for the excellent performance shown in Fig. 3c. Figure 3d demonstrates that the performance can be improved only slightly when the shaper is updated to account for the actual on-orbit system modes.

Figure 4 illustrates the experimental (solid line) and simulated (dashed line) frequency response magnitude of the MACE configuration 1 test article for the one-gimbal task. In this plot, both

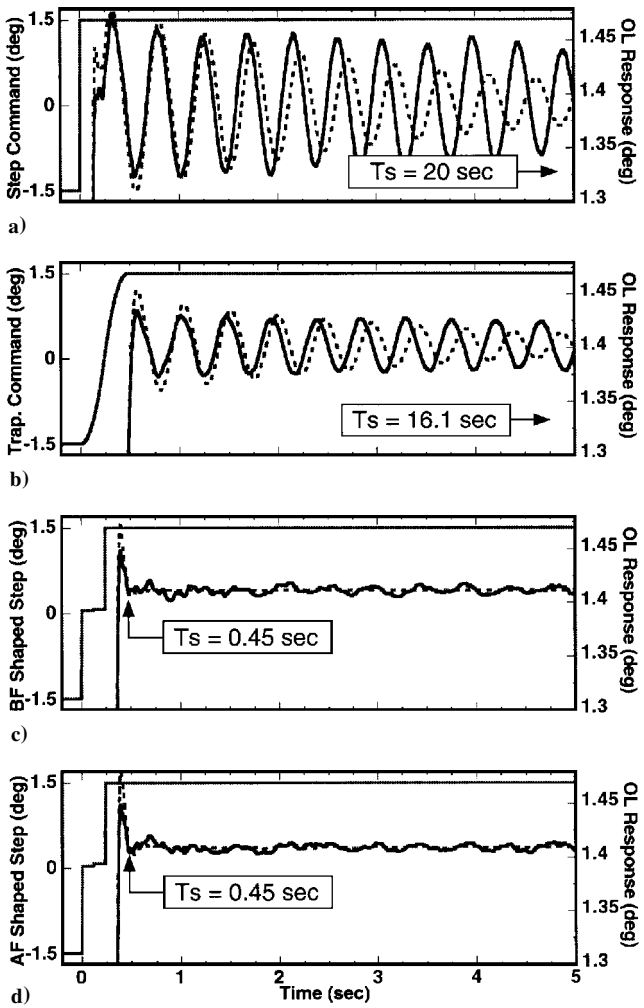

Fig. 3 Time-response results for the configuration 1, one-gimbal task.

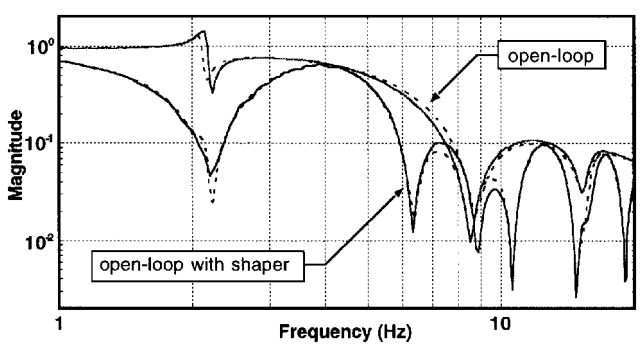

Fig. 4 Frequency-response results for the configuration 1, one-gimbal task.

the open-loop frequency response and the open-loop frequency response with the same 1-mode, ZV input shaper from Fig. 3d are shown. The experimental data in this plot were collected using a white noise input command, and the simulated data were generated using the measurement model developed after the on-orbit system ID. By comparing the unshaped to the shaped transfer function in this figure, it can be observed that the input shaper suppresses vibration by greatly reducing the amount of energy seen by the system around the first mode of 2.19 Hz. As an artifact of the input shaping algorithm, the transfer function magnitude is also reduced at regular intervals along the frequency axis. By comparing the experimental and simulated data in Fig. 4, it can also be seen that the model predictions matched closely with the experimental performance. Because the input shapers were derived using modal information from the MACE models, the excellent performance of the shaped commands in Fig. 3 can be largely attributed to this model accuracy.

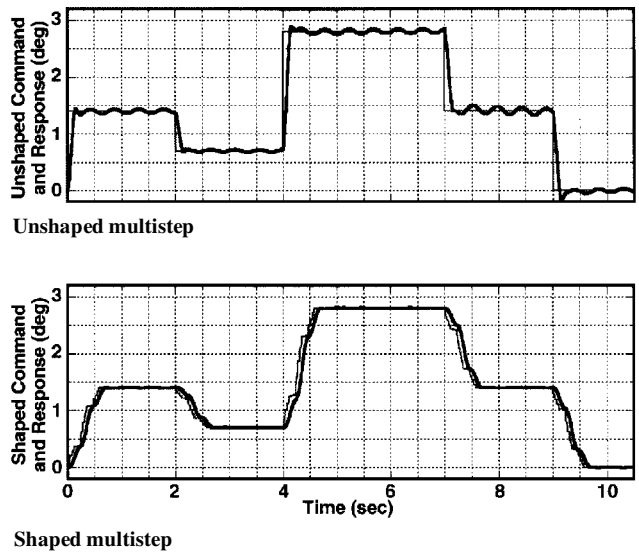

Fig. 5 Time-response results for a slewing maneuver.

To give an example of the effectiveness of input shaping for a more realistic input command, Fig. 5 illustrates the shaped and unshaped time response for a multiple-step gimbal slewing maneuver. This command profile could be used, for example, to position a satellite instrument through a series of pointing coordinates. As the first plot in Fig. 5 demonstrates, substantial vibration is excited every time the gimbal locates to a new setpoint using an unshaped command. If pointing accuracy is essential to the performance of the satellite instrument, several seconds or perhaps even minutes must pass before this vibration decays to acceptable levels. For the shaped command, however, Fig. 5 illustrates that, at the cost of a small delay in move time, the instrument can be moved to a new setpoint with almost no vibration.

In addition to the data shown in Figs. 3–5, several other shaped inputs were evaluated on-orbit. From these experiments, it was observed that single-mode input shapers provided the best performance for the configuration 1, one-gimbal task. Because the second mode of the test article in configuration 1 is above 7 Hz and most of the energy in the input commands occurs at low frequencies, little energy in the slewing commands was available to excite higher modes. From the multiple-mode shapers evaluated during the mission, it was observed that the additional modes in the shaper formulation added a small delay in the rise time of the system response while providing only a negligible improvement in the residual vibration reduction.

Several experiments were also run during the MACE mission to evaluate the advantages of increasing the robustness of the shaped commands to modal uncertainty. From these results, it was observed that, for the specified settling accuracy used in these tests, input shapers with minimal, i.e., ZV, robustness provided the best performance. Many shapers with higher-order robustness were also implemented, but due to the accuracy of the MACE models, the extra robustness did not reduce residual vibration appreciably and only added an undesirable lag to the shaped command profiles. For systems that have tighter accuracy requirements or greater uncertainty, increased robustness may become critical for keeping vibration within acceptable levels.

C. Configuration 2 Results

The results from the MACE configuration 2, one-gimbal task are shown in Figs. 6 and 7. In a format similar to Fig. 3, Fig. 6 illustrates the time response of the primary gimbal that results from three different motion commands: a step command (Fig. 6a), a shaped step designed BF (Fig. 6b), and a shaped step designed after a flight system ID was performed (Fig. 6c). In each of these three plots, both the input command and the experimental response are shown as solid lines and the predicted open-loop response is shown as a dashed line. For each test, the input command is designed to slew the gimbal by 4 deg relative to the bus, and the resulting response of the gimbal, as measured as an absolute angle, is slightly less than this.

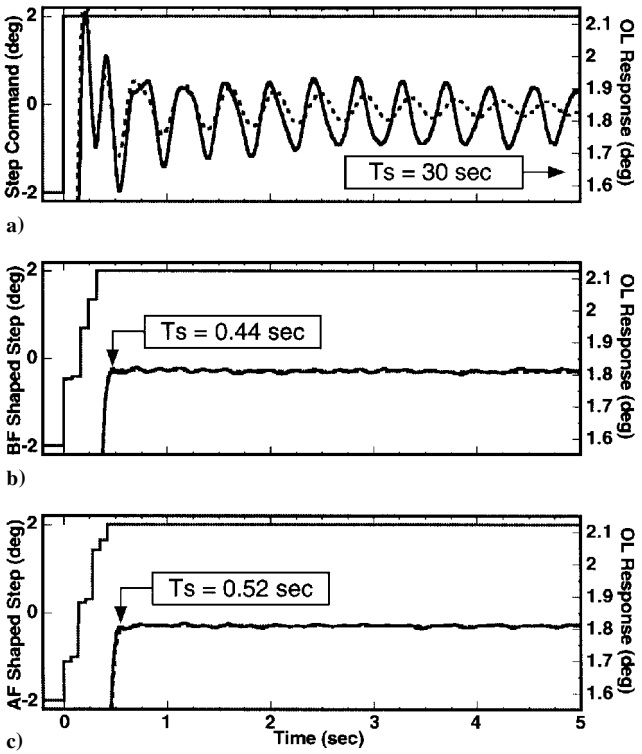

Fig. 6 Time-response results for the configuration 2, one-gimbal task.

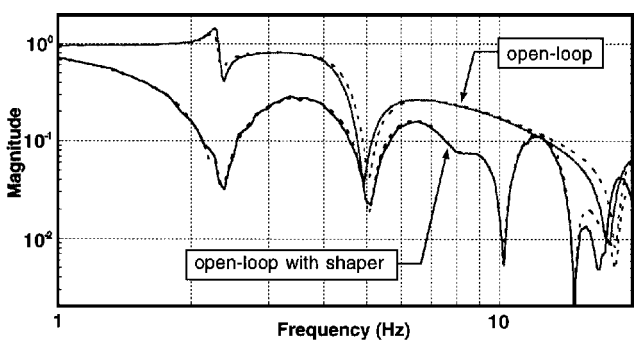

Fig. 7 Frequency-response results for the configuration 2, one-gimbal task.

As was the case with the configuration 1 results, Fig. 6a shows that, due to the lightly damped, low-frequency vibration that is excited by the step command, the pointing performance of the primary gimbal is greatly compromised. A fast Fourier transform of this time-domain data reveals that the vibration in the response appears predominantly at the first two system modes: 2.28 and 4.39 Hz. Consequently, the shaped command in Fig. 6b employs a two-mode ZV shaper derived from FEM frequency estimates made prior to flight. As a result of this shaped command, the residual vibration is dramatically reduced and the settling time is improved over the unshaped response by about a factor of 60.

By comparing the on-orbit experimental data with the simulated predictions for configuration 2 of the test article, it was found during the mission that the first two modes varied by less than 3% from their predicted values. Given this small frequency discrepancy, simply updating the two-mode ZV shaper to account for the new frequencies would provide little performance improvement. Instead, because the vibration in response to the shaped step designed BF (Fig. 6b) appeared predominantly at the second mode, the input shaper was redesigned to include ZV robustness at the first mode and extra robustness at the second mode. The resulting response to this updated shaped command (Fig. 6c) demonstrated slightly lower residual vibration but a longer settling time due to the shaper delay introduced by the added robustness at the second mode.

Similarly to Fig. 4, Fig. 7 illustrates the experimental and simulated frequency response magnitude for configuration 2 of the MACE test article. The experimental data in this plot were collected using a white noise input command, and the simulated data were generated using the FEM developed prior to flight. From the open-loop response, the first mode at 2.28 Hz is clearly visible; the second mode at 4.39 Hz, on the other hand, is obscured by a neighboring zero and by the fact that it is more heavily damped. The shaped response is for the two-mode ZV shaper designed prior to flight, and not surprisingly, this shaper effectively reduces the transfer function magnitude around the first two system modes. As was the case for configuration 1, because model predictions match closely the experimental data in Fig. 7, the excellent performance of the shaped commands derived from this model is not surprising.

V. Results for the MACE Two-Gimbal Task

A. Experiment Description

As described in Sec. III, the two-gimbal task involves slewing the MACE secondary gimbal while a MIMO controller tries to maintain the pointing angle of the primary gimbal. In these tests, a shaped or unshaped input command is sent to the secondary gimbal z-axis actuator servo while the absolute angular rate of the primary gimbal z axis, as measured by the rate gyro, is used to record the system response. Additionally, to monitor the structural vibration present in the test article during each experiment, the z-axis strain gauge on the bus link nearest the secondary gimbal was used to record the strain in the bus. This section presents and discusses the results of these experiments for both MACE configurations 1 and 2. For all of these results, the settling time of the gimbal angular rate is evaluated based on an envelope of ± 0.4 deg/s around the final value, and the settling time of the bus strain is evaluated using an envelope of ± 0.0002.

B. Configuration 1 Results

Figures 8–10 illustrate the results for a typical set of two-gimbal tests that employ a single controller and shaped command. The controller used in this set of results is a medium- to high-authority sensitivity-weighted LQG controller (as described in Ref. 6) that was designed based on actual flight ID data. The input shaper used in these tests is a two-mode, ZV shaper also designed during the mission using the on-orbit system ID data.

Figure 8 illustrates the time response of the primary gimbal in response to slew of the secondary gimbal for three different cases: the open-loop (OL) response to a step command (Fig. 8a), the

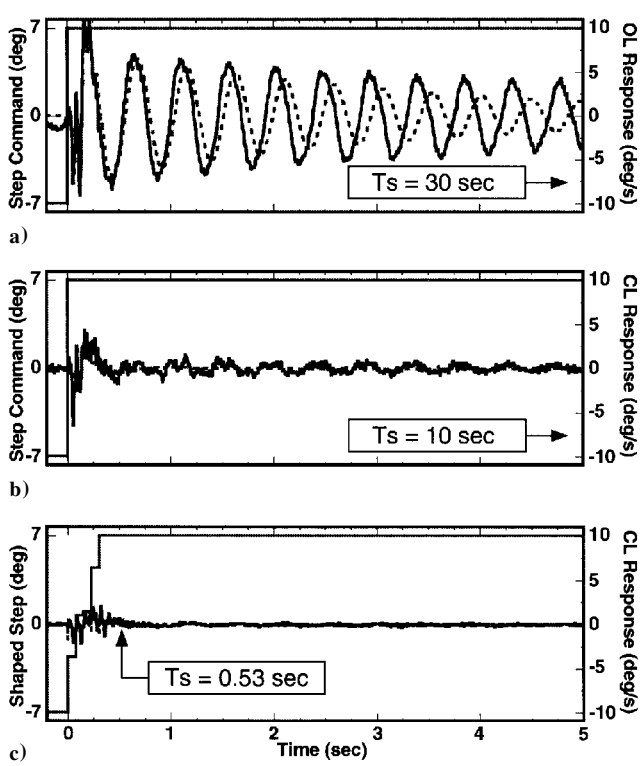

Fig. 8 Time-response results for the configuration 1, two-gimbal task.

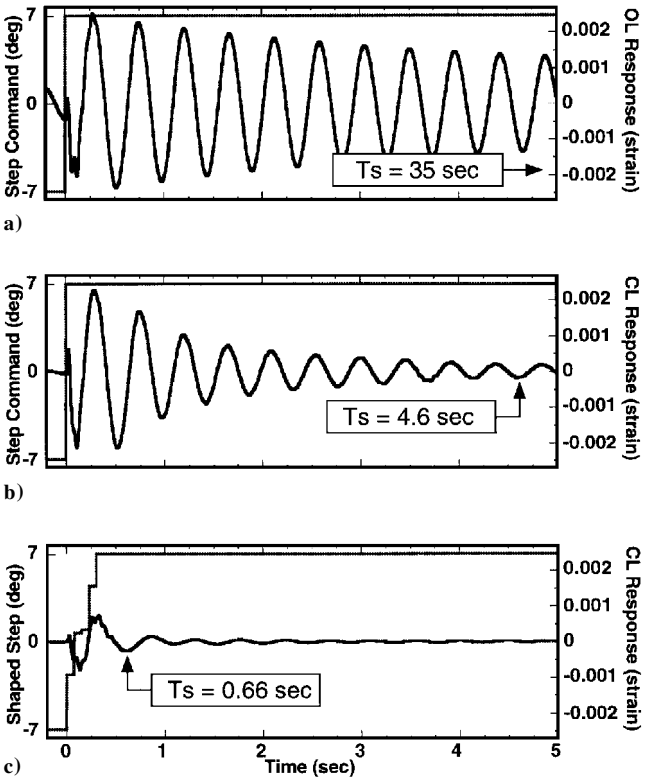

Fig. 9 Measured bus strain for the same three trials shown in Fig. 8.

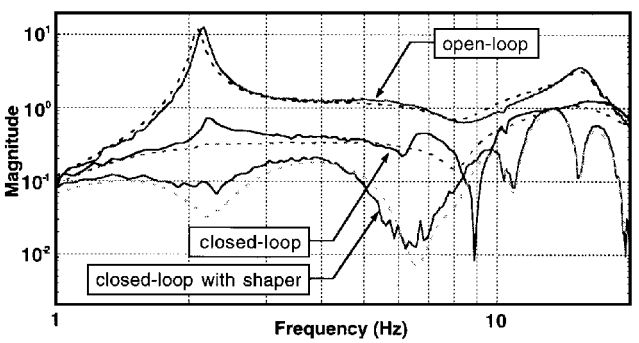

Fig. 10 Frequency-response results for the configuration 1, two-gimbal task.

closed-loop (CL) response to a step command (Fig. 8b), and the CL response to a shaped step command (Fig. 8c). In each of the three plots, the input command and experimental response are shown as solid lines and the predicted response is shown as a dashed line. Note that in the OL case, the gimbal servos remain active, and in the CL cases, the high-performance structural controller is used as well. It can be seen that the controller greatly reduces the vibration levels and settling time of the primary gimbal. The remaining vibration occurs primarily at the first two lightly damped system modes of 2.24 and 6.60 Hz. Consequently, when a two-mode shaper targeting these frequencies is added to the controlled system, the residual vibration and settling time can be further reduced (Fig. 8c).

Figure 9 illustrates the time response of the bus strain for the same three trials in Fig. 8. It can be seen that substantial vibration is excited in the MACE structure by the step command. With the controller active, this vibration is somewhat reduced. However, because the controller was not designed to reduce bus vibration, potentially problematic vibration levels exist in the structure, which might corrupt the performance of other instruments on the bus. As Fig. 9c illustrates, the addition of a shaper to the controlled system provides a simple and effective way to quiet structural vibration and improve performance.

Figure 10 illustrates the experimental and simulated frequency response magnitude for the three cases shown in Fig. 8. The experimental data were collected by measuring the response of the primary gimbal to a white noise disturbance at the secondary gimbal. The simulated data were generated using the FEM developed prior to flight, for the OL case, or the measurement model derived from actual flight data, for the other two cases. By comparing the three sets of data, it can be seen that the controller effectively reduces vibration levels over the OL, and the shaper improves the response further. By comparing the experimental data to the simulated data in this plot, it can be seen that, in the OL case, the FEM proves to be an accurate predictor of the actual on-orbit behavior. In particular, the model predicts the first bending mode to be at 2.11 Hz, whereas the actual data reveal it to be at 2.24 Hz. For the CL case, the simulation also shows fairly good agreement with the mission data. However, around the first and second modes, 2.2 and 6.6 Hz, the experimental response shows some remaining residual vibration that was not captured in the CL predictions. Because the shaper was designed to suppress vibration around these two lightly damped CL modes, this residual vibration is greatly reduced in the shaped response.

In addition to the results shown in Figs. 8–10, several other two-gimbal experiments were run on-orbit to evaluate different controllers and shapers. For instance, controllers with a range of authority were tested, and it was noticed that the performance advantages afforded by input shaping ranged from very substantial, for low-authority controllers, to slight, for the highest-authority controllers. Additionally, several different types of input shapers were tested, and it was observed that either one- or two-mode shapers with minimal robustness delivered the best performance. Given the prescribed settling band and the high accuracy of the model, shapers with additional modes or robustness reduced residual vibration levels very little but added a noticeable delay to the system response. Last, experiments were run using shapers and controllers designed both before and after flight ID data were collected. Because the FEM used to make the flight predictions was very accurate, the experiments designed before flight delivered excellent performance. As a result, upon redesign during flight, only a small performance improvement for the two-gimbal task could be achieved.

C. Configuration 2 Results

In addition to the configuration 1 experiments, a few experiments for the two-gimbal task were performed on MACE configuration 2. Similarly to the results for the one-gimbal task in Sec. IV, because the configuration 2 model was comparably accurate to the configuration 1 model, the observations made from the configuration 2 experiments were almost identical to those for configuration 1.

VI. Summary of Results and Conclusions

Based on the results of the input shaping experiments for both the one-gimbal and two-gimbal tasks, a few significant points can be summarized.

1) For the one-gimbal task, the shaped commands effectively reduced residual vibration resulting from slewing maneuvers.

2) For the two-gimbal task, the shaped commands always aided controller performance, and for the controllers with medium to low authority, this performance improvement was substantial.

3) In both the OL and CL cases, the input shapers that delivered the best performance were either one- or two-mode shapers with minimal robustness.

4) In general, the performance predicted prior to flight using the MACE FEMs agreed very closely with the experimental results for both configurations 1 and 2.

5) Because of the accuracy of the MACE 0-*g* FEMs for both configurations 1 and 2, the on-orbit redesign afforded only slight performance improvements over the shaped commands that were designed prior to flight.

6) Despite the lack of ground-based model verification for configuration 2, the FEM for configuration 2 was comparably accurate to the configuration 1 model, and, as a result, the performance of the input shaping experiments for configurations 1 and 2 was also comparable.

From these results, it can be concluded that input shaping is a simple and effective strategy for reducing vibration in flexible space structures. It can be used by itself or with CL control techniques

to enhance the performance of satellite systems with slewing and pointing instruments. Additionally, if careful ground-based modeling procedures are followed, results indicated that it is possible to achieve excellent and predictable performance in 0 *g* without conducting an on-orbit redesign.

References

[1]Miller, D. W., deLuis, J., Stover, G., and Crawley, E. F., "MACE: Anatomy of a Modern Control Experiment," *Proceedings of the International Federation of Automatic Control World Congress* (San Francisco, CA), Vol. 4, International Federation of Automatic Control, Laxenburg, Austria, 1996, pp. 31–36.

[2]Glaese, R. M., and Miller, D. W., "Derivation of 0-G Structural Control Models From Analysis and 1-G Experimentation," AIAA Paper 95-1121, April 1995.

[3]Glaese, R., and Liu, K., "On-Orbit Modeling and Identification for MACE," *Proceedings of the International Federation of Automatic Control World Congress* (San Francisco, CA), Vol. 4, International Federation of Automatic Control, Laxenburg, Austria, 1996, pp. 37–43.

[4]Liu, K., Jacques, R. N., and Miller, D., "Frequency Domain Structural System Identification by Observability Range Space Extraction," *Proceedings of the 1994 American Control Conference* (Baltimore, MD), Vol. 1, American Automatic Control Council, Evanston, IL, 1994, pp. 107–111.

[5]How, J., Glaese, R., Grocott, S., and Miller, D., "Finite Element Model Based Robust Controllers for the MIT Middeck Active Control Experiment (MACE)," *Proceedings of the American Control Conference* (Baltimore, MD), Vol. 1, American Automatic Control Council, Evanston, IL, 1994, pp. 272–277.

[6]Grocott, S. C. O., How, J. P., and Miller, D. W., "A Comparison of Robust Control Techniques for Uncertain Structural Systems," *Proceedings of the AIAA Guidance, Navigation, and Control Conference* (Scottsdale, AZ), AIAA, Washington, DC, 1994, pp. 261–271.

[7]Campbell, M. E., Grocott, S. C. O., and How, J. P., "Overview of Closed Loop Results for MACE," *Proceedings of the International Federation of Automatic Control World Congress* (San Francisco, CA), Vol. 4, International Federation of Automatic Control, Laxenburg, Austria, 1996, pp. 49–54.

[8]Farrenkopf, R. L., "Optimal Open-Loop Maneuver Profiles for Flexible Spacecraft," *Journal of Guidance and Control*, Vol. 2, No. 6, 1979, pp. 491–498.

[9]Swigert, C. J., "Shaped Torque Techniques," *Journal of Guidance and Control*, Vol. 3, No. 5, 1980, pp. 460–467.

[10]Turner, J. D., and Junkins, J. L., "Optimal Large-Angle Single-Axis Rotational Maneuvers of Flexible Spacecraft," *Journal of Guidance and Control*, Vol. 3, No. 6, 1980, pp. 578–585.

[11]Singer, N. C., and Seering, W. P., "Preshaping Command Inputs to Reduce System Vibration," *Journal of Dynamic Systems, Measurement and Control*, Vol. 112, March 1990, pp. 76–82.

[12]Magee, D. P., and Book, W. J., "Eliminating Multiple Modes of Vibration in a Flexible Manipulator," *Proceedings of the IEEE International Conference on Robotics and Automation* (Atlanta, GA), Vol. 2, Inst. of Electrical and Electronics Engineers, New York, 1993, pp. 474–479.

[13]Tzes, A. P., Englehart, M. J., and Yurkovich, S., "Input Preshaping with Frequency Domain Information for Flexible-Link Manipulator Control," *Proceedings of the AIAA Guidance, Navigation, and Control Conference* (Boston, MA), Vol. 2, AIAA, Washington, DC, 1989, pp. 1167–1175.

[14]Singhose, W., Derezinski, S., and Singer, N., "Extra-Insensitive Shapers for Controlling Flexible Spacecraft," AIAA Paper 94-3665, Aug. 1994.

[15]Singh, T., and Vadali, S. R., "Robust Time-Optimal Control: A Frequency Domain Approach," *Journal of Guidance, Control, and Dynamics*, Vol. 17, No. 2, 1994, pp. 346–353.

[16]Liu, Q., and Wie, B., "Robust Time-Optimal Control of Uncertain Flexible Spacecraft," *Journal of Guidance, Control, and Dynamics*, Vol. 15, No. 3, 1992, pp. 597–604.

[17]Rogers, K., "Limiting Vibrations in Systems with Constant Amplitude Actuators Through Command Shaping," M.S. Thesis, Dept. of Mechanical Engineering, Massachusetts Inst. of Technology, Cambridge, MA, May 1994.

[18]Banerjee, A. K., "Dynamics and Control of the WISP Shuttle-Antennae System," *Journal of Astronautical Sciences*, Vol. 41, No. 1, 1993, pp. 73–90.

[19]Singer, N. C., and Seering, W. P., "An Extension of Command Shaping Methods for Controlling Residual Vibration Using Frequency Sampling," *Proceedings of the IEEE International Conference on Robotics and Automation* (Nice, France), Vol. 1, Inst. of Electrical and Electronics Engineers, New York, 1992, pp. 800–805.

[20]Hyde, J. M., and Seering, W. P., "Using Input Command Pre-Shaping to Suppress Multiple Mode Vibration," *Proceedings of the IEEE International Conference on Robotics and Automation* (Sacramento, CA), Vol. 3, Inst. of Electrical and Electronics Engineers, New York, 1991, pp. 2604–2609.

[21]Chang, K. W., "Shaping Inputs to Reduce Vibration in Flexible Space Structures," M.S. Thesis, Dept. of Mechanical Engineering, Massachusetts Inst. of Technology, Cambridge, MA, May 1992.

[22]Singhose, W., Seering, W., and Singer, N., "Residual Vibration Reduction Using Vector Diagrams to Generate Shaped Inputs," *Journal of Mechanical Design*, Vol. 116, June 1994, pp. 654–659.

[23]Tuttle, T. D., and Seering, W. P., "A Zero-Placement Technique for Designing Shaped Inputs to Suppress Multiple-Mode Vibration," *Proceedings of the American Control Conference* (Baltimore, MD), Vol. 3, American Automatic Control Council, Evanston, IL, 1994, pp. 2533–2537.

[24]Tuttle, T. D., and Seering, W. P., "Vibration Reduction in 0-g Using Input Shaping on the MIT Middeck Active Control Experiment," *Proceedings of the American Control Conference* (Seattle, WA), Vol. 2, American Automatic Control Council, Evanston, IL, 1995, pp. 919–923.